Eur. Phys. J. B **57**, 411–422 (2007)
DOI: 10.1140/epjb/e2007-00190-7

THE EUROPEAN PHYSICAL JOURNAL B

Soliton patterns and breakup thresholds in hydrogen-bonded chains

A.S. Tchakoutio Nguetcho[1,a] and T.C. Kofane[1,2,b]

[1] Laboratoire de Mécanique, Département de Physique, Faculté des Sciences, Université de Yaoundé I, B.P. 812, Yaoundé, République du Cameroun
[2] The Abdus Salam International Centre for Theoretical Physics, P.O. Box 586 Strada Costiera, II-34014 Trieste, Italy

Received 23 October 2006 / Received in final form 4 June 2007
Published online 13 July 2007 –

Abstract. The dynamics of protons in hydrogen-bonded quasi one-dimensional networks are studied using a diatomic lattice model of protons and heavy ions including a ϕ^4 on-site substrate potential. It is shows that the model with linear and nonlinear coupling of the quartic type between lattice sites for the protons admits a richer dynamics that cannot be produced with linear couplings alone. Depending on two types of physical boundary conditions, namely of the drop or condensate type, and on conditions requiring the presence of linear and nonlinear dispersion terms, soliton patterns of compact support, whether with a peak, drop, bell, cusp, shock, kink, bubble or loop structure, are obtained within a continuum approximation. Phase trajectories as well as analytical studies provide information on the disintegration of soliton patterns upon reaching some critical values of the lattice parameters. The total energies of soliton patterns are computed exactly in the continuum limit. We also show that when anharmonic interactions of the phonon are taken into account, the width and energy of soliton patterns are in qualitative agreement with experimental data.

PACS. 62.30.+d Mechanical and elastic waves; Vibrations – 63.20.-e Phonons in crystal lattices – 05.45.Yv Solitons – 63.20.Ry Anharmonic lattice modes

1 Introduction

Transport of protons in hydrogen-bonded systems is a topic of great research interest, aiming to describe nonlinear solitonic excitations which, according to the ideas of Antonchenko, Davydov and Zolotaryuk [1], would be related to the formation and propagation of ionic and Bjerrum defects. In fact these ideas have successfully been tested in a variety of organic as well as inorganic materials which form chains, networks and solids utilizing hydrogen-bonding mechanisms, such as for example Ice and hydrogen halides which are the best known examples of inorganic hydrogen-bonded solids [2–4], whereas proteins, DNA, and other biological macromolecules are examples of organic hydrogen-bonded chains [5,6]. Protonic conductivity is usually associated with motion along a hydrogen-bonded chain of ionic(ionization) and Bjerrum (orientational or bonding) defects [4,7]. The former involve translational motions of the hydrogen-bonded protons, whereas the latter are results of rotations of the hydroxyl ions or some other hydroxyl groups. Transport of protons may begin either with the passage of an ionic defect or the passage of an orientational defect, but thereafter the motion of these defects must strictly alternate [5,6,8,9]. Furthermore, it has been demonstrated that many biological activities, such as photosynthesis, repair mechanisms of DNA after radiation damage, metabolism, signal transduction in cells, enzymatic processes, and respiration which are driven by electron transfer reactions [10,11], may proceed along a single pathway which, as the preferred channel for electron transfer reactions, can be established by a hydrogen-bonded strand within the secondary structure [12,13].

One of the questions that has been raised for the mechanism of proton conductivity concerns the roles played by the nonlinear on-site potential for the protons, leading to three possible scenarios: (1) the model usually consists of two interacting sublattices: one of harmonically coupled light ions(protons) with a doubly degenerate nonlinear on-site potential of the ϕ^4 type and the other of harmonically coupled heavy ions. Theories differ in choosing the form of the interaction between the two sublattices. Usually, a nonlinear coupling between the two sublattices is considered [14,15], although there are models which consider a linear coupling [16,17]; (2) the doubly

[a] e-mail: nguetchoserge@yahoo.fr
[b] e-mail: tckofane@yahoo.com

degenerate nonlinear on-site potential is of the double-Morse type. In fact, as shown by quantum chemistry calculations [18–20], a good approximation of the double-well potential can be constructed as the superposition of two symmetrically positioned ion-proton Morse potentials as well as an ion-ion coupling [21–29]; (3) the nonlinear on-site potential is of the double sine-Gordon type with nonlinear [30,31] and linear [32] couplings. In the first two cases, models are able to describe energy transport, dielectric polarization, and proton storage in hydrogen-bonded networks but they are unable to explain the protonic mass in such a system which is required in order to support the saturated protonic conductivity in ice and other hydrogen-bonded semiconductors [33]. In the last case, models can explain simultaneously the ionic and Bjerrum defects formation and propagation using well-known soliton properties [30–32,32]. Besides the nonlinear on-site potential for the protons, hydrogen-bonded models with phonon anharmonisms occur as well. Such a model was first introduced by adding higher-order terms such as the cubic and quartic anharmonicities to the harmonic potential [34–39,39]. Later, an exponential nonlinearity was considered, represented by, e.g., Morse, Toda or Lennard-Jonnes potentials [40–44].

As is well-known, the solitons existing in these models result from the balanced competition between dispersion and nonlinear effects. Recently, it has been shown that the inclusion of anharmonicities in the study of lattice models can produce qualitatively new effects. In particular, Rosenau and Hyman [45] found solutions of the solitary type without infinite tails, termed solitons with compact support or compactons [46–51]. In other words, two adjacent compactons do not interact unless they come into contact in a way similar to the contact between hard spheres. It has been shown that the effects of lattice discreteness, and the presence of a linear coupling between lattice sites are detrimental to a stable ballistic propagation of the compacton, because of the particular structure of the small oscillation frequency spectrum of the compacton in which the lower frequency internal modes enter in direct resonance with phonon modes [48]. The existence of a localized breathing mode with compact support has been demonstrated [48]. A quantization condition on the value of the width parameter of the discrete compacton has been proposed [47].

The aim of this paper is to investigate the properties of the one-dimensional diatomic chain of protons and heavy ions, where the proton dynamics is influenced by anharmonic lattice vibrations. Except for the work by Kashimori et al. [37], our anharmonic treatment of the lattice vibrations goes beyond the usual harmonic approximation of a two-sublattice soliton model of the hydrogen-bonded proton Hamiltonians [1,30,33]. In the model with quartic nonlinear proton-proton coupling to be discussed, conditions are considered that require the presence of nonlinear dispersion as well as linear dispersion. In this paper we show that soliton pattern mechanisms that require a nonlinear coupling of the protons in adjacent hydrogen bonds may exist if one properly chooses a class of physical boundary conditions. The obtained patterns are solitons of compact support, without infinite tails rather than the kinks with infinite tails in the coupled double-well model.

The paper is organized as follows. In Section 2, the model Hamiltonian of one-dimensional interacting two-sublattice model of anharmonically coupled protons and harmonically coupled heavy ions is presented. Using two types of physical boundary conditions, namely the "zero" or nonvanishing classes of boundary conditions, in the continuum limit two-component compactonlike solutions are obtained and their total energies are calculated. Analytic expressions for the dependence of the breakdown threshold value on the nonlinear parameter, on the constant coupling between the two sublattices, and on the velocity of the soliton patterns are derived. The last section contains a summary and conclusions.

2 The model and analytical results

2.1 The model

In the study of proton transfer processes in hydrogen-bonded systems, it is usual to consider one dimensional chains, the so-called Bernal-Fowler filaments [1,2,27,52,53], which consist of two coupled sublattices $\cdots X-H\cdots X-H\cdots X-H\cdots X-H\cdots$, where the hydrogen atom H (or proton H^+) with mass m in each lattice unit is connected to its adjacent heavy ions or more generally hydroxyl groups X or (X^-) via either a covalent $(-)$ or a hydrogen $(\cdots)$ bond of mass M $(m<M)$, forming a hydrogen bonded bridge $X-H\cdots X$ [1,37]. The covalent and hydrogen bonds in a $X-H\cdots X$ configuration are interchangeable, viz., the proton in the bond that links the two X ions together can tunnel between two equilibrium positions which are energetically approximately equivalent. In such a case, the two-dimensional intrabond proton potential is assumed to be a symmetric double-well function of a general form with two minima. This double well potential is also motivated physically by considering the simultaneous electromagnetic interaction of the two proton neighbour heavy ions (details on the structure of this potential are given in Refs. [54,55]). A typical example of such a potential for the proton in the hydrogen bond is the well-known double-well potential [1]:

$$V\left(u_n\right)=V_0V_{\mathrm{sub}}\left(u_n\right), \tag{1}$$

with

$$V_{\mathrm{sub}}\left(u_n\right)=\left(1-\frac{u_n^2}{u_0^2}\right)^2, \tag{2}$$

where u_n denotes the displacement of the nth proton with respect to the center of the heavy-ion pair, V_0 the potential barrier, and $2u_0$ [the two minima $(\pm u_0,0)$ correspond to the degenerate ground states of the chain] is the distance between the two minima of the double-well potential, as illustrated in Figure 1.

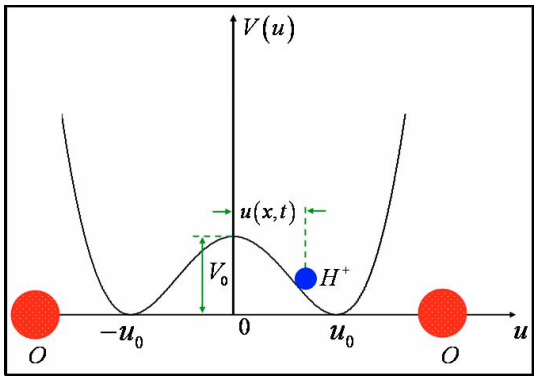

Fig. 1. A symmetric double well potential for the proton in a hydrogen bond of the chain.

Generally, it is not possible to provide a double-well form of the intrabond proton potential within a standard diatomic chain, using only nearest-neighbour interactions. Therefore some additional interactions with appropriate parameters, forbidding the adjacent heavy ions to approach each other very close, should be included. For archetypal simplicity of the $2C$ model, it is sufficient to impose either, (i) an external, single-well on-site potential for each heavy ion of the chain, periodically located at a sufficiently large distance or instead; (ii) a nearest-neighbor coupling between adjacent heavy ions with sufficient strength and large equilibrium distance between them. Thus in order to describe still better these physical phenomena in the hydrogen-bonded chains, there exist other types of double-well potentials such as the Double-sine one used by Pnevmatikos [30] or the Double-Morse one placed tail-to-tail used by Karpan et al. [27]. In addition these potentials possess the characteristic of taking account of the variations both in the height of the double well potential and in the position of its minima. However with these potentials, it is very difficult to have analytic solutions. The advantage of the ϕ^4 potential that we use is that not only is it possible to obtain analytical solutions in the continuum limit, but also that this model proves to be of relevance for the description of proton transfer in hydrogen bonds [52,53].

The total Hamiltonian of the system is:

$$H = H_1 + H_2 + H_3, \tag{3}$$

where the Hamiltonian of the proton sublattice [37] is:

$$H_1 = \sum_n \left[\frac{1}{2} m \left(\frac{du_n}{dt} \right)^2 + V(u_n) + \frac{1}{2} m C_0^2 (u_{n+1} - u_n)^2 + \frac{1}{4} m C_a (u_{n+1} - u_n)^4 \right], \tag{4}$$

in which the two last terms represent the harmonic and anharmonic couplings, respectively, with C_0 the characteristic velocity and C_a the anharmonic coupling parameter between neighbouring protons.

For what concerns the state and motion of the heavy ion in our model, we use simply a harmonic oscillator with low frequency acoustic-vibration, on account of the large mass associated to a large number of atoms or atomic groups. Thus the Hamiltonian of the heavy-ion sublattice is [52,53,55,56]

$$H_2 = \sum_n \frac{1}{2} M \left(\frac{dy_n}{dt} \right)^2 + \frac{1}{2} M v_0^2 (y_{n+1} - y_n)^2, \tag{5}$$

where the last term describes an harmonic coupling between neighbouring heavy ions pairs.

The last contribution to the total Hamiltonian H of our model arises from the dynamical interaction between the two sublattices and describes the modulation of the double well potential caused by the variation of the distance between the heavy ions that surround the proton. This energy can be measured experimentally or estimated from approximated theoretical expressions [56]. The shape that we use is proposed by Braun et al. [60,61]. It takes into account the interactions between the relative movements of atoms in two chains. It can also describe interactions between donors and acceptors [1,55]. In the discrete lines of Josephson transmission, it describes the inductive coupling [56]. The interacting Hamiltonian is given by:

$$H_3 = \sum_n \chi (y_{n+1} - y_n) (u_0^2 - u_n^2), \tag{6}$$

where χ measures the strength of the coupling between the two interacting sublattices. From the total Hamiltonian, one can derive, in dimensionless form, the equations of motion as follows:

$$m \left(\frac{d^2 u_n}{dt^2} \right) = m C_0^2 (u_{n+1} + u_{n-1} - 2u_n) - V_0 \frac{dV_{\text{sub}}(u_n)}{du_n} + m C_a \left[(u_{n+1} - u_n)^3 + (u_{n-1} - u_n)^3 \right] + 2\chi u_n (y_{n+1} - y_n) \tag{7}$$

$$M \left(\frac{d^2 y_n}{dt^2} \right) = m v_0^2 (y_{n+1} + y_{n-1} - 2y_n) + \chi (u_{n-1} - u_n)(u_{n-1} + u_n). \tag{8}$$

Equations (7) and (8) are not solvable analytically. By assuming that the coupling between neighboring sites is sufficiently strong, the discrete variables $u_n(t)$, and $y_n(t)$ can be replaced by two continuous functions of space and time $u(x = na, t)$, $y(x = na, t)$, and under this continuum approximation, equations (7) and (8) become,

$$m \left(\frac{d^2 u}{dt^2} \right) = m a^2 C_0^2 \left(\frac{d^2 u}{dx^2} \right) + 3 m a^4 C_a \frac{d^2 u}{dx^2} \left(\frac{du}{dx} \right)^2 + 2a\chi u \left(\frac{dy}{dx} \right) - V_0 \frac{dV_{\text{sub}}(u)}{du} \tag{9}$$

$$M \left(\frac{d^2 y}{dt^2} \right) = M a^2 v_0^2 \left(\frac{d^2 y}{dx^2} \right) - 2a\chi u \left(\frac{du}{dx} \right) \tag{10}$$

where a is the lattice parameter.

2.2 Soliton excitations

We now turn our attention to possible travelling wave solutions. For the sake of convenience, we can look for solutions with fixed profile moving at a constant velocity v. Thus in the moving frame and as a function of the moving dimensionless variable $s = \dfrac{x - vt}{a}$, equations (9) and (10) yield,

$$\left[1 - V_1^2 + 3C_{nl}\left(\frac{du}{ds}\right)^2\right]\left(\frac{d^2u}{ds^2}\right) = \lambda\frac{dV_{\rm sub}\,(u)}{du} - 2\chi_1 u\left(\frac{dy}{ds}\right) \quad (11)$$

$$\left(1 - V_2^2\right)\left(\frac{d^2y}{ds^2}\right) = 2\chi_2 u\left(\frac{du}{ds}\right) \quad (12)$$

where $V_1 = \dfrac{v}{aC_0}$ and $V_2 = \dfrac{v}{av_0}$ are the scaled (dimensionless) soliton velocities of protons and heavy-ions, respectively. $C_{\rm nl}$ is the parameter that controls the strength of the nonlinear coupling and is related to the anharmonic coupling coefficient C_a by the relation $C_{\rm nl} = \dfrac{C_a}{C_0^2}$, while $\chi_1 = \dfrac{\chi}{mC_0^2}$ and $\chi_2 = \dfrac{\chi}{Mv_0^2}$ are the parameters that control the strength of the coupling between the two interacting sublattices. Finally $\lambda = \dfrac{V_0}{mC_0^2}$ denotes the scaled amplitude of the periodic potential and measures the effective depth of the proton potential. Integrating equation (12), one obtains

$$\frac{dy}{ds} = \frac{\chi_2}{(1 - V_2^2)}u^2 + K_1 \quad (13)$$

where K_1 is a constant of integration determined from the boundary conditions. Two types of boundary conditions are being used, namely the trivial or the classical classes of boundary conditions.

2.2.1 Soliton excitations with "zero" type boundary conditions

"zero" boundary conditions are appropriate for drop and peak soliton solutions [51], and are defined by the expressions

$$\frac{du}{ds} \longrightarrow 0, \quad u \longrightarrow 0, \quad as \quad s \longrightarrow \pm\infty$$
$$\frac{dy}{ds} \longrightarrow 0, \quad as \quad s \longrightarrow \pm\infty. \quad (14)$$

Considering equation (13) with these boundary conditions equation (14) substituted into equation (11), one obtains

$$\left[1 - V_1^2 + 3C_{nl}\left(\frac{du}{ds}\right)^2\right]\left(\frac{d^2u}{ds^2}\right) = \lambda\frac{dV_{\rm sub}\,(u)}{du} - \frac{2\chi_1\chi_2}{(1 - V_2^2)}u^3. \quad (15)$$

The solutions of equation (15) can best be analyzed in the phase plane $\left(u, \dfrac{du}{ds}\right)$. Thus, equation (15) can be treated as an autonomous dynamical system given by

$$\frac{dp}{du} = \frac{1}{p\,(1 - V_1^2 + 3C_{nl}p^2)}\left[\lambda\frac{dV_{\rm sub}\,(u)}{du} - \frac{2\chi_1\chi_2}{(1 - V_2^2)}u^3\right] \quad (16)$$

where the derivative $p = \dfrac{du}{ds}$, describes the elongation of the energy bonds in the system. The first integral of this equation, describing the phase portraits of the dynamical system [see equation (7)], may easily be obtained with the boundary condition given by equation (14) and can be written as [52]

$$p^4 - 2p_0^2p^2 = \alpha\left(u^4 - 2\beta u^2\right) \quad (17)$$

where $p_0 = \sqrt{\dfrac{V_1^2 - 1}{3C_{\rm nl}}}$, $\alpha = \dfrac{4\lambda\left(V_2^2 + \eta - 1\right)}{3C_{\rm nl}u_0^4\left(V_2^2 - 1\right)}$, $\beta = \dfrac{u_0^2\left(V_2^2 - 1\right)}{V_2^2 + \eta - 1}$ with $\eta = \dfrac{\chi_1\chi_2u_0^4}{2\lambda}$. It is clear from the nonlinear equation (17) that the system carries out symmetrical oscillations of low amplitude around the single stable equilibrium point $(0, 0)$, when $\eta > 1$ with $V_2 \in]0; 1[$, or when $\eta < 1$ with $V_2 \in]V_{22}; 1[$, where $V_{22} = \sqrt{1 - \eta}$, and for positive values of $C_{\rm nl}$. In such case, there is no double-well potential. There is only one minimum of the potential and thus no localized soliton solution exists in this case.

But when $C_{\rm nl} < 0$, this stable position is transformed into an unstable one, and any perturbation of the system can induce destruction of the structure.

For $\eta > 1$ and $V_2 \in]1; \infty[$, or for $\eta < 1$ and $V_2 \in]0; V_{22}[\cup]1; \infty[$, the system admits three equilibrium positions including two unstable ones $\left[\left(-\sqrt{\beta}, 0\right)\right.$ and $\left.\left(\sqrt{\beta}, 0\right)\right]$, and one stable one at $(0, 0)$. Thus, the system carries out oscillations of low amplitude around the single stable equilibrium point $(0, 0)$. Beyond certain upper-bound values of the amplitude, unlimited motions occur, leading to the destruction of the system. However, when $C_{\rm nl}$ takes a negative value, under the same conditions the system can carry out two types of oscillations: oscillations of small amplitude around the stable points $\left(-\sqrt{\beta}, 0\right)$ and $\left(\sqrt{\beta}, 0\right)$, or oscillations of very large amplitude until reaching the two stable positions. When $C_{\rm nl}$ increases upon reaching the threshold value

$$C_{\rm nl_{cr1}} = \frac{\left(V_2^2 + \eta - 1\right)\left(V_1^2 - 1\right)^2}{12\lambda\left(V_2^2 - 1\right)}, \quad (18)$$

the phase portraits change qualitatively. Indeed, singular points are almost present in the phase plane plots. One can note the disappearance of the separatrix, indicating the disintegration of soliton solutions. As one can readily see from equation (18), the associated threshold values depend on the soliton velocities of protons and heavy-ions, the nonlinear parameter and on the effective depth of the proton potentials. In order to solve equation (17), we introduce the following condition

$$\left(V_2^2 + \eta - 1\right)\left(1 - V_1^2\right)^2 - 12\lambda C_{\rm nl}\left(V_2^2 - 1\right) = 0 \quad (19)$$

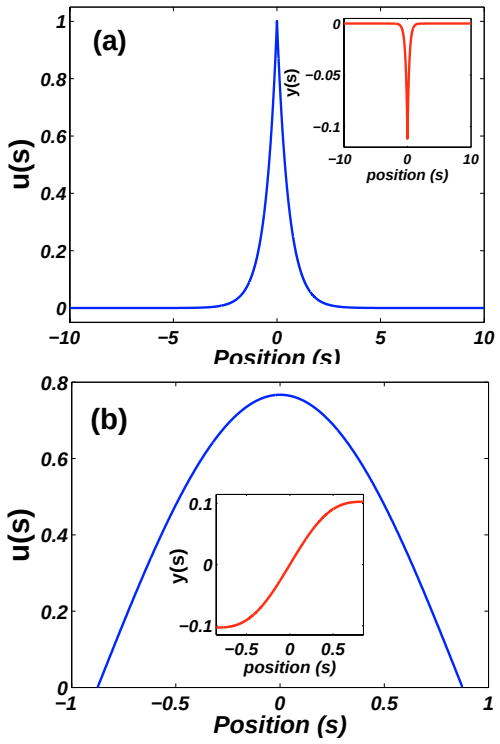

Fig. 2. Representation of the field of two-component compact solutions u (for the proton) and y (for the hydroxyl) as a function of the position s, corresponding to the waveforms: (a) the peak solitons (peakons) and (b) the drop solitons, according to equations (20) and (22) respectively, with the condition equation (19) for $\eta = 3$, $u_0 = 1$, $V_2 = 1.5$, $V_1 = 1.5$, $s_0 = 0$, $C_{nl} = 0.44$, $\chi 2 = 1$ and $\lambda = 1$

for which soliton patterns are available. After some lengthy algebra, analytical solutions have been obtained which for the sake of clarity are presented in the following manner.

2.2.1.1 Peak solitons (peakons)

These solutions appear when equation (17) is solved using equation (19). For the motion of the proton, the solution describing a single peak soliton defined by merging the two solution branches is:

$$u = \exp\left[\pm\frac{p_0}{\sqrt{\beta}}(s - s_0)\right]. \tag{20}$$

The solution for the heavy-ions motion can easily be obtained by inserting equation (20) into equation (13) and using the boundary conditions (14), leading to

$$y = \pm\frac{\chi_2\sqrt{\beta}}{4p_0(1 - V_2^2)}\exp\left[\pm\frac{2p_0}{\sqrt{\beta}}(s - s_0)\right]. \tag{21}$$

Graphs representing these solutions are depicted in Figure 2a.

2.2.1.2 Drop compactons

This terminology is introduced to designate solutions that usually have the form of hump solitons but are defined now over a compact support in space and which, because of their form and properties, are reminiscent of hard spheres [51]. The proton waveform is given by

$$u = \pm\sqrt{2\beta}\sin\left[\frac{p_0}{\sqrt{\beta}}(s - s_0)\right] \tag{22}$$

and the heavy-ion waveform is given by

$$y = \frac{\beta\chi_2}{2(V_2^2 - 1)}\left[(s - s_0) - \frac{\sqrt{\beta}}{2p_0}\sin\left[\frac{2p_0}{\sqrt{\beta}}(s - s_0)\right]\right]. \tag{23}$$

Figure 5b presents the double solution for the two sublattices. The width of this drop soliton can be evaluated and has the form

$$L_{drop} = \pi\frac{\sqrt{\beta}}{p_0}.$$

By taking into account equation (19), it was obvious to notice that this width of the drop soliton is independent of the anharmonicity parameter $C_{\rm nl}$ and the coupling parameter of the two sublattices χ. However, this width increases with the speed V_1 of the proton particles and decreases with the effective depth λ of the substrate potential. We also notice that the amplitude of this type of wave varies with the propagation velocity V_2 of the heavy-ions and the coupling parameter χ (for a fixed value of V_2, the amplitude decreases when the coupling strength between the two sublattices increases). Hereafter, the energy of these configurations is evaluated. The total energy of these soliton patterns can be calculated by inserting the explicit solutions into the expression for the Hamiltonian density, that is:

$$E_{\rm total} = mC_0^2E_1 + Mv_0^2E_2 + \chi E_3 \tag{24}$$

with

$$\begin{aligned}
E_1 &= \int_{-\infty}^{+\infty}\left[\frac{1}{2}\left(1 + V_1^2\right)\left(\frac{du}{ds}\right)^2\right. \\
&\quad \left. + \frac{1}{4}C_{\rm nl}\left(\frac{du}{ds}\right)^4 + \lambda V_{\rm sub}\left(u\right)\right] ds, \\
E_2 &= \int_{-\infty}^{+\infty}\frac{1}{2}\left(1 + V_2^2\right)\left(\frac{dy}{ds}\right)^2 ds, \\
E_3 &= \int_{-\infty}^{+\infty}\left(u_0^2 - u^2\right)\left(\frac{dy}{ds}\right) ds.
\end{aligned} \tag{25}$$

By using the above expression, while taking into account of equation (19), we obtain:

$$\begin{aligned}
E_1 &= \frac{p_0u_0^2\left(1 + V_1^2\right)}{2\sqrt{\beta}} + \frac{C_{\rm nl}p_0^3u_0^4}{8\beta^{\left(\frac{3}{2}\right)}} \\
&\quad - \frac{\lambda u_0^2\sqrt{\beta}\left(u_0^2 - 4\beta\right)}{2p_0} \\
E_2 &= \frac{u_0^4\chi_2^2\sqrt{\beta}\left(1 + V_2^2\right)}{4p_0\left(1 - V_2^2\right)^2} \\
E_3 &= \frac{\chi_2u_0^4\sqrt{\beta}}{2p_0\left(1 - V_2^2\right)}
\end{aligned} \tag{26}$$

for the peak soliton and,

$$E_1 = \frac{p_0\left(1+V_1^2\right)}{\sqrt{\beta}}\left[u_0\sqrt{\beta-u_0^2}+\beta\arcsin\left(\frac{u_0}{\sqrt{\beta}}\right)\right] + \frac{C_{\rm nl}p_0^3}{2\beta^{\left(\frac{3}{2}\right)}}\left[2u_0\left(\beta-u_0^2\right)^{\left(\frac{3}{2}\right)}+3u_0\beta\sqrt{\beta-u_0^2}\right] + 3\beta^2\arcsin\left(\frac{u_0}{\sqrt{\beta}}\right)$$

$$E_2 = \frac{\chi_2^2\left(1+V_2^2\right)\sqrt{\beta}}{p_0\left(V_2^2-1\right)^2}\left[3\beta^2\arcsin\left(\frac{u_0}{\sqrt{\beta}}\right) -2u_0^3\sqrt{\beta-u_0^2}-3u_0\beta\sqrt{\beta-u_0^2}\right]$$

$$E_3 = \frac{2\chi_2\beta^{\left(\frac{3}{2}\right)}}{p_0\left(V_1^2-1\right)}\left[3u_0\beta\sqrt{\beta-u_0^2} + \left(2u_0^2-3\beta\right)\arcsin\left(\frac{u_0}{\sqrt{\beta}}\right)\right] \quad (27)$$

for the drop soliton, respectively.

2.2.2 Soliton excitations with nonvanishing boundary conditions

The nonvanishing boundary conditions are defined by the relation

$$\frac{du}{ds}\longrightarrow 0,\quad u\longrightarrow u_{\min},\quad as\quad s\longrightarrow\pm\infty$$
$$\frac{dy}{ds}\longrightarrow 0,\quad as\quad s\longrightarrow\pm\infty. \quad (28)$$

where $u_{\min}$ is the minimum of the substrate potential $V(u)$. These boundary conditions are appropriated for kink, cusp, peak, and shock soliton solutions. Substituting equation (13) with the condition (28) into equation (11), one obtains,

$$\frac{d^2u}{ds^2} = \frac{1}{\left[1-V_1^2+3C_{\rm nl}\left(\frac{du}{ds}\right)^2\right]}\left[\lambda\frac{\partial V_{\rm sub}(u)}{\partial u} -\frac{2\chi_1\chi_2}{\left(1-V_2^2\right)}u\left(u^2-u_{\min}^2\right)\right]. \quad (29)$$

The first integral of equation (29), describing the phase portraits of the dynamical system, may easily be obtained and is given by the relation

$$p^4-2p_0^2p^2=\alpha\left(u_0^2-u^2\right)^2. \quad (30)$$

From (30) and when $V_2\neq V_{22}$, classical equilibrium points (corresponding to the extrema of the potential and characteristic for the harmonic interparticle potential system) will always exist. When $\eta>1$ with $V_2\in\,]0;1[$, or when $\eta<1$ with $V_2\in\,]V_{22};1[$, the dynamic behavior of the system is described by a limited bistable potential. On the other hand, when $\eta>1$ with $V_2\in\,]1;\infty[$, or when $\eta<1$ with $V_2\in\,]0;V_{22}[\cup]1;\infty[$, the system can make small oscillations around $(0,0)$, and around certain values of the amplitudes one notices its rupture. All these results have been obtained for positive values of $C_{\rm nl}$. When the latter takes negative values, the bistable system becomes catastrophic and vice versa. Similarly, in the case of the trivial (drop) boundary conditions (14), the separatrix representing the soliton solutions and relating $u_{\min1}$ to $u_{\min2}$, exists for values of $C_{\rm nl}$ less than the threshold

$$C_{\rm nl_{cr2}}=\frac{\left(1-V_2^2\right)\left(1-V_1^2\right)^2}{12\lambda\left(V_2^2+\eta-1\right)}, \quad (31)$$

and goes away for values of $C_{\rm nl}$ larger than the latter.

Besides these points, a few more singular points appear for the drop and nonvanishing types of boundary conditions when $V_1\in\,]1;\infty[$ and $C_{\rm nl}>0$, or when $V_1\in[0;1]$ and $C_{\rm nl}<0$. The exact position of these new points may be derived from the singularity arising in the denominator of equations (16) and (29). These new points have exactly, under the same conditions as previously, X-coordinates identical to those obtained previously. The main difference is the addition of two new ordinates $-p_0$ and p_0 (the characteristic impulse of the system) besides the one given by $p=0$. When the model parameters satisfy the relation:

$$\left(V_2^2-1\right)\left(1-V_1^2\right)^2+12\lambda C_{\rm nl}\left(V_2^2+\eta-1\right)=0 \quad (32)$$

the implicit solutions describing proton displacement can be written as:

$$\pm\frac{\sqrt{2}p_0}{u_0}\left(s_{ltn}-s_0\right)=\arcsin\left(\frac{l}{\sqrt{2}}\frac{u}{u_0}\right) + \ln\left[t\sqrt{1-\frac{1}{2}\left(\frac{u}{u_0}\right)^2}+\frac{n}{\sqrt{2}}\frac{u}{u_0}\right] \quad (33)$$

where ln is the neperian logarithm, $l=\pm1$, $t=\pm1$, $n=\pm1$, these symbols simply indicating the sign of each denoted term on the right-hand side of equation (33), and s_0 is defined by the chosen initial condition. According to equation (28), we have four pairs of defined boundary conditions and each pair produces two branches to construct the solutions. Since each branch of the solution travels with the same velocity, the necessary gap Δ in the space s for coalescing solutions, determined by the initial conditions, can be presented in the two types [$\Delta_1=0$ and $\Delta_2=\arcsin(1)$]. Let us first take some solutions when they merge in the "space" with Δ_2. For the boundary condition

$$u\to-u_0 \text{ while } s\to-\infty, \text{ and } u\to u_0 \text{ while } s\to\infty, \quad (34)$$

the solitonic structure can be defined by

$$\frac{\sqrt{2}p_0}{u_0}\left(s_{+--}+\frac{\pi}{2}\right)\ \text{ if }\ \frac{\sqrt{2}p_0}{u_0}s\in\,]-\infty,0],$$
$$\text{and }\ -\frac{\sqrt{2}p_0}{u_0}\left(s_{--+}-\frac{\pi}{2}\right)\ \text{ if }\ \frac{\sqrt{2}p_0}{u_0}s\in[0,\infty[.$$

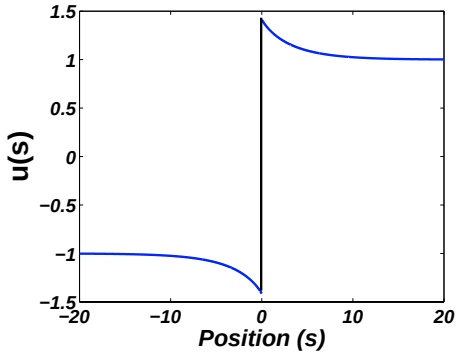

Fig. 3. Representation of the field of soliton solutions u (for the proton) as a function of the position s, corresponding to the waveforms of the shock waves (because of the abrupt discontinuities that are observed when they are traveling). According to equation (33) with the boundary condition equation (34) for $s_0 = 0$, $m = 1$, $M = 16$, $v_0 = 2$, $C_0 = 1/5$, $\chi = 1.752$, $\lambda = 3/5$ and $u_0 = 1$.

This relation, displayed in Figure 3 is usually referred to as a shock wave, has an energy given by equation (24) with

$$\begin{aligned} E_1 &= \sqrt{2}\left(\frac{1}{2}-\frac{\pi}{8}\right)\left(1+V_1^2\right)u_0p_0 \\ &\quad+\frac{\sqrt{2}C_{\mathrm{nl}}u_0p_0^3}{8}\left(\frac{5}{2}-\frac{3\pi}{4}\right) \\ &\quad+\frac{\sqrt{2}u_0\lambda}{p_0}\left(\frac{3}{4}-\frac{\pi}{8}\right), \\ E_2 &= \frac{\sqrt{2}u_0^5\chi_2^2\left(1+V_2^2\right)(6-\pi)}{16p_0\left(V_2^2-1\right)^2}, \\ E_3 &= \frac{\sqrt{2}\chi_2u_0^5(6-\pi)}{8p_0\left(V_2^2-1\right)}. \end{aligned} \tag{35}$$

For the boundary condition

$$u \to -u_0 \text{ while } s \to -\infty, \text{ and } u \to -u_0 \text{ while } s \to \infty, \tag{36}$$

the solitonic structure can be defined by

$$\frac{\sqrt{2}p_0}{u_0}\left(s_{-++}+\frac{\pi}{2}\right) \text{ if } \frac{\sqrt{2}p_0}{u_0}s \in \left]-\infty,\frac{\pi}{2}\right],$$
$$\text{and} -\frac{\sqrt{2}p_0}{u_0}\left(s_{-++}+\frac{\pi}{2}\right) \text{ if } \frac{\sqrt{2}p_0}{u_0}s \in \left[-\frac{\pi}{2},\infty\right[.$$

$$\frac{\sqrt{2}p_0}{u_0}\left(s_{+++}-\frac{\pi}{2}\right) \text{ if } \frac{\sqrt{2}p_0}{u_0}s \in \left]-\infty,0\right],$$
$$\text{and} -\frac{\sqrt{2}p_0}{u_0}\left(s_{+++}-\frac{\pi}{2}\right) \text{if} \frac{\sqrt{2}p_0}{u_0}s \in [0,\infty[.$$

The first pair is a loop soliton (see Fig. 4a) whose energy is divergent and the second is another wave which represents a peak soliton (see Fig. 4b), whose energy is given

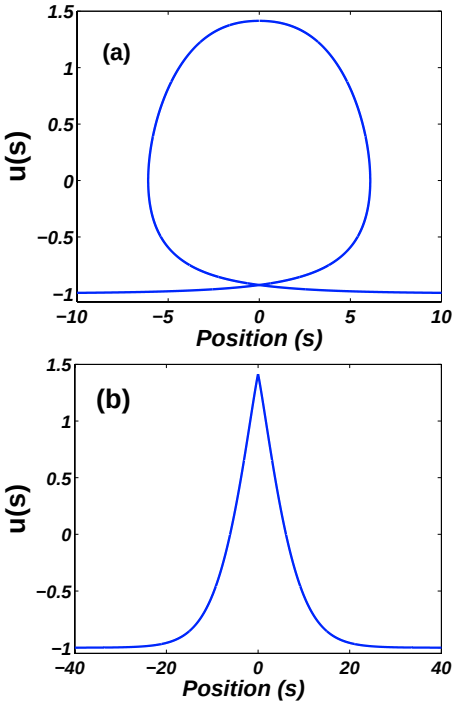

Fig. 4. Representation of the field of soliton solutions u (for the proton) as a function of the position s, corresponding to the waveforms: (a) Loop soliton and (b), Typical peak soliton, according to equation (33) with the boundary condition equation (36) for $s_0 = 0$, $m = 1$, $M = 16$, $v_0 = 2$, $C_0 = 1/5$, $\chi = 1.752$, $\lambda = 3/5$ and $u_0 = 1$.

by equation (24), with

$$\begin{aligned} E_1 &= \sqrt{2}\left(\frac{3\pi}{8}+\frac{1}{2}\right)\left(1+V_1^2\right)u_0p_0 \\ &\quad+\frac{\sqrt{2}C_{\mathrm{nl}}u_0p_0^3}{8}\left(\frac{5}{2}+\frac{9\pi}{4}\right) \\ &\quad+\frac{3\sqrt{2}u_0\lambda}{p_0}\left(\frac{1}{4}+\frac{\pi}{8}\right), \\ E_2 &= \frac{3\sqrt{2}u_0^5\chi_2^2\left(1+V_2^2\right)(2+\pi)}{16p_0\left(V_2^2-1\right)^2}, \\ E_3 &= \frac{3\sqrt{2}\chi_2u_0^5(2+\pi)}{8p_0\left(V_2^2-1\right)}. \end{aligned} \tag{37}$$

Let us now consider the case where solutions are specially obtained by coalescing two branches of each pair solution in equation (33), for the second type of nonzero gap Δ_1. For the boundary condition

$$u \to u_0 \text{ while } s \to -\infty, \text{ and } u \to u_0 \text{ while } s \to \infty, \tag{38}$$

the solitonic structure can be defined by

$$\frac{\sqrt{2}p_0}{u_0}s_{-+-} \text{ if } \frac{\sqrt{2}p_0}{u_0}s \in \left]-\infty,0\right],$$
$$\text{and} -\frac{\sqrt{2}p_0}{u_0}s_{-+-} \text{ if } \frac{\sqrt{2}p_0}{u_0}s \in [0,\infty[,$$

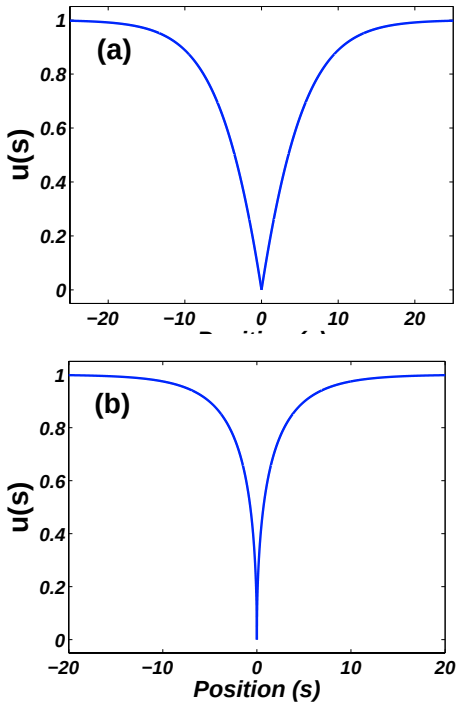

Fig. 5. Representation of the field of bubble soliton solutions u (for the proton) as a function of the position s, corresponding to the waveforms, (a) Peak bubble (because of its rarefied form in the center) and (b) , Cusp solitons in the form of a straight bubble directed down that is an acute dip in the condensate according to equation (33) with the boundary condition equation (38) for $s_0 = 0$, $m = 1$, $M = 16$, $v_0 = 2$, $C_0 = 1/5$, $\chi = 1.752$, $\lambda = 3/5$ and $u_0 = 1$.

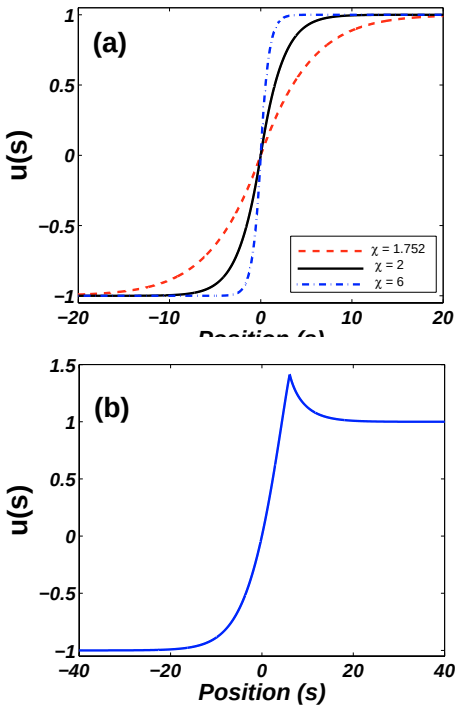

Fig. 6. Representation of the field of soliton solutions u (for the proton) as a function of the position s, corresponding to the waveforms of the typical kinklike structure for different value of parameter of coupling of the two sublattices χ (a), and the kink soliton with small hump near its center (b), according to equation (33) with the boundary condition equation (34) for $s_0 = 0$, $m = 1$, $M = 16$, $v_0 = 2$, $C_0 = 1/5$, $\chi = 1.752$, $\lambda = 3/5$ and $u_0 = 1$.

$$\frac{\sqrt{2}p_0}{u_0}s_{++-} \text{ if } \frac{\sqrt{2}p_0}{u_0}s \in]-\infty, 0],$$
$$\text{and} -\frac{\sqrt{2}p_0}{u_0}s_{++-} \text{ if } \frac{\sqrt{2}p_0}{u_0}s \in [0, \infty[\,.$$

The corresponding pattern structures are plotted in Figure 5, and exist as excitations in a condensed state, like a rarefaction of the field. Their forms suggest the names peak bubble and cusp bubble, respectively.

The energy of the peak bubble is given by equation (24), with

$$E_1 = \frac{\pi\sqrt{2}\left(1+V_1^2\right)u_0p_0}{8} + \frac{3\sqrt{2}C_{\rm nl}u_0p_0^3}{16}\left(\frac{\pi}{2}-1\right) + \frac{\sqrt{2}u_0\lambda}{8p_0}\left(6+\pi\right), \quad (39)$$
$$E_2 = \frac{\sqrt{2}u_0^5\chi_2^2\left(1+V_2^2\right)\left(6+\pi\right)}{16p_0\left(V_2^2-1\right)^2},$$
$$E_3 = \frac{\sqrt{2}\chi_2u_0^5\left(6+\pi\right)}{8p_0\left(V_2^2-1\right)},$$

whereas the energy of the cusp diverges.

For the boundary condition given by equation (34), the solutions are

$$\frac{\sqrt{2}p_0}{u_0}s_{+++} \text{ if } \frac{\sqrt{2}p_0}{u_0}s \in]-\infty, 0]\,,$$
$$\text{and} -\frac{\sqrt{2}p_0}{u_0}s_{-+-} \text{ if } \frac{\sqrt{2}p_0}{u_0}s \in [0, \infty[$$

$$\frac{\sqrt{2}p_0}{u_0}s_{+++} \text{ if } \frac{\sqrt{2}p_0}{u_0}s \in \left]-\infty, \frac{\pi}{2}\right],$$
$$\text{and} -\frac{\sqrt{2}p_0}{u_0}s_{--+} \text{ if } \frac{\sqrt{2}p_0}{u_0}s \in \left[\frac{\pi}{2}, \infty\right[,$$

and are represented in Figure 6.

These are topological kink-like solitons, solutions very often used to interpret and to explain the process of the transfer of protons in hydrogen-bonded systems. The second one has a little peak near the center and can be interpreted as a domain travelling along the medium. The energy of kink-like solitons, which consists of kinetic and potential terms, can be calculated from equation (24),

with

$$E_1 = \frac{\pi\sqrt{2}u_0 p_0}{8}\left(1+V_1^2\right) + \frac{3\left(\pi-2\right)\sqrt{2}u_0 p_0^3 C_{\rm nl}}{32} + \frac{\sqrt{2}\left(\pi+6\right)\lambda}{8p_0} \quad (40)$$

$$E_2 = \frac{\left(6+\pi\right)\sqrt{2}\chi_2^2 u_0^5}{16p_0\left(1-V_2^2\right)}\left(1+V_2^2\right)$$

$$E_3 = \frac{\left(4+\pi\right)\sqrt{2}\chi_2 u_0^5}{4p_0\left(V_2^2-1\right)}\left(1+V_2^2\right)$$

and for the kink-like solitons and

$$E_1 = \sqrt{2}u_0 p_0\left(1+V_1^2\right)\left(\frac{\pi}{8}+\frac{1}{2}\right) + \frac{\sqrt{2}u_0 p_0^3 C_{\rm nl}}{16}\left(5+\frac{3\pi}{2}\right) + \frac{\sqrt{2}u_0\left(\pi+6\right)\lambda}{8p_0} \quad (41)$$

$$E_2 = \frac{\left(6+\pi\right)\sqrt{2}\chi_2^2 u_0^5}{16p_0\left(V_2^2-1\right)}\left(1+V_2^2\right)$$

$$E_3 = \frac{\left(6+\pi\right)\sqrt{2}\chi_2 u_0^5}{8p_0\left(V_2^2-1\right)}\left(1+V_2^2\right)$$

for the kink solitons with small hump near the center.

The width L of the kink-like soliton (shown in Fig. 6a) is estimated at 99% and is given by

$$L = \frac{\sqrt{2}u_0}{p_0}\left[\arcsin\left(\frac{\sqrt{2}u_1}{2u_0}\right) + \ln\left(\frac{1}{2}\sqrt{4-2\left(\frac{u_1}{u_0}\right)^2}+\frac{\sqrt{2}u_1}{2u_0}\right)\right] \quad (42)$$

where $u_1 = \frac{99}{100}u_0$. Since equation (42) shows that the width of the kinks increases with the anharmonicity, the present one will be able to only decrease with a strong coupling of the two sublattices (shown in Fig. 10a). For example, let us estimate the width of the compacton kink solution. Small displacements of the protons around the equilibrium position involve a weak proton-proton interaction, on the order of a tenth of the force constant of the covalent bond of the OH. But when the displacement of the proton is large the interaction becomes strong, and the term $\frac{1}{4}mC_a\left(u_{n+1}-u_n\right)^4$ becomes the dominant contribution. As an example in the case of the structure of ice, proton transfer can be illustrated in a one dimensional frame for the water molecules chain, in which a proton migrates from a water molecule to another to form an ionic defect, a hydroxonium, H_30^+, and another water molecule is dissociated by losing one of its protons to its neighbors, forming a hydroxyl, $0H^-$. Each proton (H^+) can be transferred inside the $X-H\ldots X$ bridge interchanging the role of the covalent ($-$) and the hydrogen ($\ldots$) bonds with the heavy ion group (X). After such an intrabond proton transfer, the chain is locally disturbing its neutral charge distribution and generates an ionic defect. However, it is possible that an additional degree of freedom allows the group ($X-H$) to rotate in an interbond proton transfer which generates a bonding (Bjerrum or orientational) defect and which restores the chain to its original state. This clearly shows that there are two distinct types of mechanisms of proton transferred in the hydrogen-bonded systems. Any of the two defects could be the majority charge carried through the chain. Both types of defects are also sensitive to the vibrations of the heavy ions substrates. The problem is how do the two types of defects can combine automatically and alternate spontaneously in the transfer process? It is these problems that may be solved by our model with new ideas from nonlinear dynamics and solitons motion that we use to try finding an answer to this phenomenon. The compactons (as those obtained in Figs. 6a and 4b) having properties much more interesting than soliton solutions of old models, will be able to better explain these physical phenomena. Under these conditions we obtain $L \approx 3.7$ Å. Our numerical applications are carried out for ice at $T = 263$ K (-10 °C) . At this temperature, the lengths of the $O-H$ and $H\ldots O$ bonds are, respectively, 1.01 Å and 1.75 Å. This gives for the lattice spacing a (e.g. the distance between two protons or two heavy-ions) the value $a = 2.76$ Å [57]. The distance u_0 along the chain from the top of the barrier to one minimum in the double well potential is $u_0 = 0.39$ Å and the barrier $V_0 = 0.74$ eV [63]. The sound velocities C_0 for the proton sublattice and v_0 for the heavy-ion sublattice have the values $C_0 = 1.1\times 10^4$ m s^{-1} and $v_0 = 0.1C_0$. The masses of the particles are $m = 1$ a.m.u (atomic mass unit) for the proton and $M = 17$ a.m.u. for the heavy-ion. We have taken the particular value $\chi = 30$ eV/Å^2 for the coupling constant and $v = 650$ m s^{-1} for the velocity. In Figure 7, we have plotted the energy of compacton solitons (see Eq. (40)) against the coupling coefficient χ. In a general way, using the two-sublatice soliton-bearing model with anharmonic interaction, the energy and the width of the kink compacton solitons, or of other types of soliton patterns that we have obtained are much smaller than those of previous models [31,37,53,57,58]. Contrary

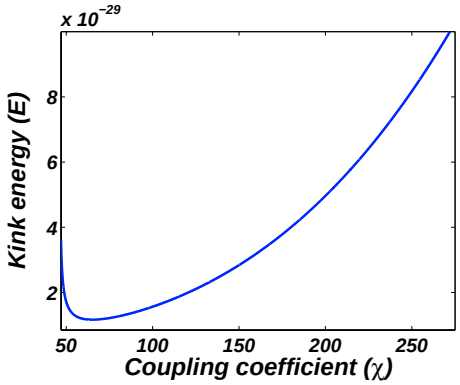

Fig. 7. Variation of the kinks energy versus χ according to equation (40) for $m = 1$ a.m.u, $M = 17$ m, $C_0 = 1.1\times 10^4$ m s^{-1}, $v_0 = 0.1C_0$, $V_0 = 0.74$ eV, $u_0 = 0.39$ and $v = 650$ m s^{-1}.

to the kink soliton in hydrogen bonded chain, or in other real physical systems which can be modelled by our system, the solutions obtained involves about one and two protons only. Therefore, the present model seems to be more realistic and applicable to a system which consist of a small number of hydrogen bonds. Amongst other, it was shown by Tchofo et al. [47] that, despite the fact that the lattice discreteness of the system have some harmful effects on the dynamics of compactons such as the existence of the Peierls-Nabarro potential which provides pinning sites for compactons or, a linear coupling which gives rise to a phonon band which enters in direct resonance with the internal modes of the compactons, causing radiation of energy away from the compactons, these types of solutions have an extraordinary capacity to execute a stable ballistic propagation in the system. These limiting factors are also strongly reduced for $Cl \simeq 0$ and $C_{nl} \gg 1$. In addition, the existence of a Goldstone mode in this parameter region makes possible a stable ballistic propagation for compactons. It was also shown by Xia et al. [81], which studied the propagation and collision of the compacton-like kinks in the system of an anharmonic discrete lattice with a double well on-site potential by direct algebraic method and numerical experiments that, the localisation of the compactons is related to the nonlinear coupling parameter C_{nl} and the potential barrier height V_0 of the double well potential, and the velocity of the propagation of the compacton is determined by the linear coupling parameter C_l, the nonlinear C_{nl} and the localisation parameter. They also show by numerical experiments that appropriate C_l is suit to a stable propagation of compacton.

It is true that all this rich variety of solutions did not have all explanations for the hydrogen bonds, the anharmonic and coupled Klein-Gordon equations having a broad field of applications, will make it possible to the scientists to improve or better to explain certain physical phenomena. These rich various types of solutions already very required and are very much used in several other models. Thus, peakons which constitute some types of solitary waves with discontinuous at the crest has been subject to attention of many physicists and mathematicians [67–69] since the pioneering work of Camassa and Holm (CH). These solutions belong to many $(1 + 1)$-dimensional nonlinear evolution equations (NEE) amongst which the CH equation describing. The waves dynamics at the free surface of fluids under gravity in the so-called shallow water approximation [70]. Recently, a novel $(1 + 1)$-dimensional nonlinear equation (NLE) known as Vakhnenko equations (VE) has been derived [71], and which models the propagation of waves in relaxing medium [72]. Morrison and Parkes [73] have investigated the generalized form of the VE and have derived types of peakon solution to this equation. Moreover, another interesting solitary waves with loop shape has been derived in many equations among which the VE [74], the generalized VE [73], the modified generalized VE [73]. It has been pointed out that the VE shares the same property with some equation recently studied by Konno and Jeffrey [74] and which models the nonlinear propagation of deformation waves in flexible long string. Another interesting application of loop-shaped solitons has been found in a system modelled by a coupled integrable dispersion equation [75] which describe the motion of a charged object in an external magnetic field. Performing this coupled equation to a weakly gravitationally field, Kuetche et al. [76] have derived the loop shaped solitons. Using some bled transformation of the independent variables, this equation has been transform to a novel one known as Schäfer-Wayne short pulse equation [77] which describes the propagation of the ultra-short pulses in Silica optical fibres. Some $(1+1)$-dimensional NLE equations have been extended to $(2 + 1)$-dimensional NLE equation in several ways [78] with many applications in hydrodynamics [79] and plasma physics [80] and others which has loops, cups, peaks and bubble soliton solutions.

3 Conclusions

In summary, we have presented a study of a nonlinear model for the motion of defects in quasi one-dimensional hydrogen-bonded systems. The model extends previous two-sublattice soliton-bearing one-dimensional models discussed in the literature, by the inclusion of anharmonicity couplings in the lattice models. This is accomplished through the introduction of a quartic proton-proton interaction potential. The presence of nonlinear and linear dispersion terms leads to soliton patterns in the continuum limit, i.e., in the limit when only long-wavelength excitations are present. It was shown that in this limit, by applying two types of boundary conditions of the "zero" or nonvanishing class, and by considering the sign of the nonlinear proton-proton coupling, a rich analytic diversity of soliton patterns emerges, namely so-called peak, drop, bell, cusp, shock, kink, bubble and loop solitons of which stability was briefly studied by the authors Agüero et al. [51], probably because of their implicit and complicated forms. The total energy of all these coupled two-component soliton patterns has been calculated and decreases with the coupling of two sublattices when the interactions of the first one are of the anharmonic form. Another effect is related to a transition from closed to open phase trajectories of the system taking place beyond some threshold value of the lattice parameter, and/or the velocity of the soliton patterns. An exact analytical expression for the dependence of the breakdown threshold value on the nonlinear parameter, the velocity of soliton and on the coupling parameter between the two sublattices, has been derived. These phenomena, for example, should contribute to the formation of cracks originating from dislocations observed in semiconductor heterostructures (more details are given in Refs. [64–66]). Impurities, as well as other defects, may locally influence the breakdown threshold and thus play a major role with respect to nonlinear excitations in such systems.

For future studies it is worth mentioning that the stability and the propagation of the solitons patterns obtained were not made in detail. A detailed study of stability for each type of solutions and their propagation, as

their applications in the hydrogen bonds would come to supplement this study. Then the situation will be more complicated because of the implicit form of the soliton solutions patterns. But we expect that such modification will not change the main finding of this investigation since in some other cases such complications have been successfully handled already. However, the problem of stability is still open. The response of the soliton in our model to an external field will be examined elsewhere, which is important for determination of physical consequences of the soliton which can be tested experimentally, such as mobility and conductivity, just as the thermal motion of the protons in the systems with finite temperature, by the transfer integral. The numerical study of two-component soliton patterns in hydrogen-bonded chains taking into account lattice discreteness [27,28,54,55] is now in progress.

One of us (T.C.K.) acknowledges financial support from the Abdus Salam International Centre for Theoretical Physics. The other (A.S.T.N.) would like to thank Professor Jan Govaerts for many helpful discussions, its materiel assistance and the encouragement, and Doctor David Yemele for helpful discussions.

References

1. V.Ya. Antonchenko, A.S. Davydov, A.V. Zolotaryuk, Phys. Status Solidi B **11**, 5, 631 (1983)
2. M. Springborg, Phys. Rev. Lett. **59**, 2287 (1987)
3. R.W. Jansen, R. Bertocini, D.A. Pinnick, A.I. Katz, R.C. Hanson, O.F. Sankey, M. O'Keeffe, Phys. Rev. B **35**, 9830 (1987)
4. P.B. Hobbs, *Ice Physics* (Clarendon, Oxford, 1974)
5. J.F. Nagle, Morowitz, Proc. Natl. Acad. Sci. USA **75**, 298 (1978)
6. J.F. Nagle, S. Tristam-Nagle, J. Membrane Biol. **74**, 1 (1983)
7. N. Bjerrum, Science **115**, 385 (1952)
8. J.F. Nagle, M. Mille, H.J. Morowitz, J. Chem. Phys. **72**, 3959 (1980)
9. E.W. Knapp, K. Schulten, Z. Schulten, Chem. Phys. **46**, 215 (1980)
10. D. Devault, *Quantum-mechanical Tunneling in Biological Systems* (Cambridge University Press, Cambridge, 1984)
11. C. Branden, J. Tooze, *Introduction to Protein Structure* (Garland, New York, 1991)
12. I.A. Balabin, J.N. Onuchic, J. Phys. Chem. **100**, 11573 (1996)
13. P.E.M. Siegbahn, M.R.A. Blomberg, R.H. Crabtree, Theor. Chem. Acc. **97**, 289 (1997)
14. A.V. Zolotaryuk, K.H. Spatschek, E.W. Laedke, Phys. Lett. A **101**, 517 (1984)
15. E.W. Laedke, K.H. Spatschek, M. Jr Wilkens, A.V. Zolotaryuk, Phys. Rev. A **32**, 1161 (1985)
16. St. Pnevmatikos, Phys. Lett. A **122**, 249 (1987)
17. S. Yomosa, J. Phys. Soc. Jpn **52**, 1866 (1983)
18. X. Duan, S. Scheiner, J. Mol. Struct. **270**, 173 (1992)
19. X. Duan, S. Scheiner, Int. J. Quantum Chem. Quantum Biol. Symp. **19**, 109 (1992)
20. X. Duan, S. Scheiner, R. Wang, Int. J. Quantum Chem. Quantum Biol. Symp. **20**, 77 (1993)
21. E.S. Kryachko, Chem. Phys. **143**, 359 (1990)
22. A.V. Zolotaryuk, St. Pnevmatikos, A.V. Savin, Physica D **51**, 407 (1991)
23. A.V. Savin, A.V. Zolotaryuk, Phys. Rev. A **44**, 8167 (1991)
24. R. Grauer, K.H. Spatschek, A.V. Zolotaryuk, Phys. Rev. E **47**, 236 (1993)
25. O. Yanovitskii, G. Vlastou-Tsinganos, N. Flytzanis, Phys. Rev. B **48**, 12645 (1993)
26. A.V. Zolotaryuk, M. Peyrard, K.H. Spatschek, Phys. Rev. E **62**, 5706 (2000)
27. V.M. Karpan, Y. Zolotaryuk, P.L. Christiansen, A.V. Zolotaryuk, Phys. Rev. E **66**, 066603 (2002)
28. V.M. Karpan, Y. Zolotaryuk, P.L. Christiansen, A.V. Zolotaryuk, Phys. Rev. E **70**, 056602 (2004)
29. G. Kalosakas, A.V. Zolotaryuk, G.P. Tsironis, E.N. Economou, Phys. Rev. E **56**, 1088 (1997)
30. St. Pnevmatikos, Phys. Rev. Lett. **60**, 1534 (1988)
31. G.P. Tsironis, St. Pnevmatikos, Phys. Rev. B **39**, 7161 (1989)
32. B. Dey, M. Daniel, J. Phys. Condens. Matter **2**, 2331 (1990)
33. E.S. Nylund, G.P. Tsironis, Phys. Rev. Lett. **66**, 1886 (1991)
34. E. Simo, T.C. Kofane Physica Scripta **49**, 543 (1994)
35. E. Simo, T.C. Kofane, Phys. Rev. E **54**, (1996)
36. A.V. Zolotaryuk, K.H. Spatschek, A.V. Savin, Phys. Rev. B **54**, 266 (1996)
37. Y. Kashimori, F. Chien, K. Nishimoto, Chem. Phys. **107**, 389 (1986)
38. Y. Zolotaryuk, J.C. Eilbeck, J. Phys. Condens. Matter **10**, 4553 (1998)
39. N.K. Voulgarakis, G.P. Tsironis, Phys. Rev. B **63**, 014302 (2000)
40. M.A. Ratner, B.G. Vekhter, Phys. Rev. B **51**, 3469 (1995)
41. D. Hennig, Phys. Rev. E **61**, 4550 (2000)
42. M.G. Velarde, W. Ebeling, A.P. Chetverikov, Int. J. Bifurcation, Chaos **15**, 245 (2005)
43. M.G. Velarde, W. Ebeling, D. Hennig, C. Neissner, Int. J. Bifurcation, Chaos **16**, 1035 (2006)
44. D. Hennig, C. Neisser, M.G. Velarde, W. Ebeling, Phys. Rev. B **73**, 024306 (2006)
45. P. Rosenau, J.M. Hyman, Phys. Rev. Lett. **70**, 564 (1993)
46. A.S. Tchakoutio Nguetcho, J.R. Bogning, D. Yemele, T.C. Kofane, Chaos, Solitons, Fractals **21**, 165 (2004)
47. P. Tchofo Dinda, T.C. Kofane, M. Remoissenet, Phys. Rev. E **60**, 7525 (1999)
48. P. Tchofo Dinda, M. Remoissenet, Phys. Rev. E **60**, 6218 (1999)
49. S. Dusuel S, P. Michaux, M. Remoissenet, Phys. Rev. E **57**, 2320 (1999)
50. Kevrekidis, V.V. Konotop, A.R. Bishop, S. Takeno, J. Phys. A. Math. Gen. **35**, L641 (2002)
51. M.A. Aguero, M.J. Paulin, Phys. Rev. E **63**, 046606 (2001)
52. X.F. Pang, H.J.W. Muller Kirsten, J. Phys., Condensed Matter **12**, 885 (1999)
53. X.F. Pang, H.W. Zhang, J. Znu, Int. J. Modern Physics B (World Scientific (Vol. 19)) **25**, 3835 (2005)
54. A.V. Zolotaryuk, M. Peyrard, K.H. Spatschek, Phys. Rev. E **62**, 5706 (2000)
55. M. Peyrard, St. Pnevmatikos, N. Flytzanis. Rev. A **36**, 903 (1987)

56. D. Hochstrasser, H. Buttner, H. Desfontaines, M. Peyrard, Phys. Rev. A **38**, 5332 (1988)
57. P. Woafo, R. Takontchoup, A.S. Bokosah, J. Chem. Phys. Solids **56**, 9, 1277 (1995)
58. R. Mefougue, P. Woafo, T.C. Kofane, Solid State Commun. **86**, 393 (1993)
59. C.M. Ngabireng, P. Woafo, T.C. Kofane, Solid State Commun. **89**, 885 (1994)
60. O.M. Braun, Y.S. Kivshar, A.M. Kosevich, J. Phys. C **21**, 3881 (1988)
61. O.M. Braun, V.K. Medvedev, Usp. Fis Nauk (Sov. Phys. Usp) **157**, 631 (1989)
62. G. Pannetier, *Chimie Physique General. Atomique. Liaisons chimiques et structures moléculaires*, 3rd edn. (Masson, 1969)
63. Xu Ji-Zhong, Solid State Commun **76**, 557 (1990)
64. P. Franzosi, G. Salviati, M. Scaffardi, F. Genova, S. Pellegrino, A. Stano, J. Cryst. Growth **88**, 125 (1988)
65. A. Milchev, Phys. Rev. B **42**, 6727 (1988)
66. A. Milchev, Physica D **41**, 262 (1989)
67. A. Parker, Y. Matsuno, J. Phys. Soc. Jpn **75**, 12401 (2006)
68. A. Constatin, J. Math. Phys. **46**, 023506 (2005)
69. Y. Matsuno, J. Phys. Soc. Jpn **76**, 034003 (2006)
70. R. Camassa, A.I. Zenchuk, Phys. Lett. A **281**, 26 (2001)
71. V.O. Vakhnenko, J. Math. Phys. **40**, 2011 (1999)
72. V.O. Vakhnenko, J. Phys A. Math. Gen. **25**, 4181 (1992)
73. A.J. Morrison, E.J. Parker, Glasgow Math. J. A **43**, 65 (2001)
74. K. Konno, A. Jeffrey, J. Phys. Soc. Jpn **52**, 1 (1983)
75. H. Kakuhata, K. Konno, J. Phys. Soc. Jpn **68**, 1 (1999)
76. V.K. Kuetche, T.B. Bouetou, T.C. Kofane, J. Phys. A. Math. Gen. **39**, 12355 (2006)
77. T. Schäfer, C.E. Wayne, Physica D **196**, 90 (2004)
78. D.J. Benney, G.J. Rokes, Stud. Appl. Maths **47**, 377 (1969)
79. M.J. Ablowitz, H. Segun, Solitons, the inverse scattering transform, Philadelphia, SIAM (1981)
80. K. Nishinari, K. Abe, I. Satsuma, J. Phys. Soc. Jpn **62**, 2021 (1993)
81. Q.L. Xia, J.H. Yi, L.Y. Li, Y.D. Peng, Chin. Phys. Soc. **14**, 0571 (2005)